



Working Paper

Stagnation point analysis

Author(s):

Fey, Michael; Jeltsch, Rolf; Müller, S.

Publication Date:

1992

Permanent Link:

<https://doi.org/10.3929/ethz-a-004283469> →

Rights / License:

[In Copyright - Non-Commercial Use Permitted](#) →

This page was generated automatically upon download from the [ETH Zurich Research Collection](#). For more information please consult the [Terms of use](#).

Stagnation point analysis ¹

M. Fey, R. Jeltsch and S. Müller ²

Research Report No. 92-03
September 1992

Seminar für Angewandte Mathematik
Eidgenössische Technische Hochschule
CH-8092 Zürich
Switzerland

¹This is an extended version of the article “Stagnation point computations of non-equilibrium inviscid blunt body flow” submitted to Computers and Fluids

²Institut für Geometrie und Praktische Mathematik, RWTH Aachen

Stagnation point analysis ¹

M. Fey, R. Jeltsch and S. Müller ²

Seminar für Angewandte Mathematik
Eidgenössische Technische Hochschule
CH-8092 Zürich
Switzerland

Research Report No. 92-03

September 1992

Abstract

The numerical solution of a symmetric hypersonic blunt body flow in two space dimensions is considered, and the problem of the arising chemical boundary layer is discussed. Analytical and numerical investigations are used to analyze the solution on the stagnation point streamline. We point out the necessary assumptions to obtain an equivalent system of ordinary differential equations along this line and to get a unique solution. We also describe the situation in the limiting case at the stagnation point and give a differential algebraic system from which we obtain the solution at this point. We derive the shape of the boundary layer by linearizing the equations. Some of our results differ from those of other authors. Then we present numerical tools to get a better indication of this boundary layer even in 2D calculations.

Keywords: chemical boundary layer, geometrical singularities

Subject Classification: 35L65, 65M99, 76K05, 76N15

¹This is an extended version of the article “Stagnation point computations of non-equilibrium inviscid blunt body flow” submitted to Computers and Fluids

²Institut für Geometrie und Praktische Mathematik, RWTH Aachen

1 Introduction

In the case of a hypersonic, inviscid continuum flow past a blunt body, a so-called bow shock (shown in Figure 1) is formed. The flow is composed of a subsonic and a hypersonic part (between the shock and the wall), separated by the sonic line. Details can be found in [2], [1].

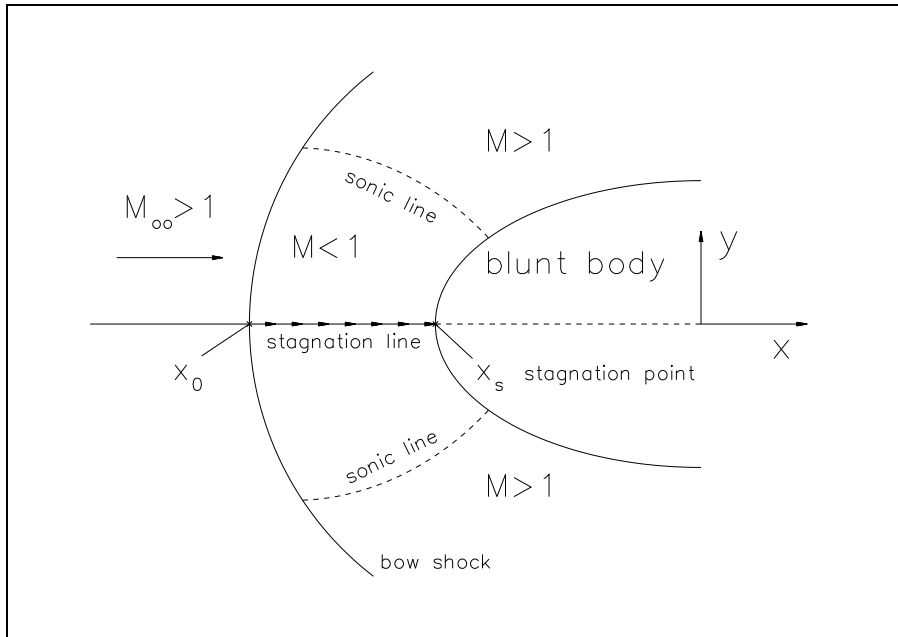


Figure 1: *Hypersonic blunt body flow*

Here we are particularly interested in

- the stand-off distance and
- the stagnation point.
- the shape of the functions near the stagnation point

In the literature there exist some investigations of the 1960s on this topic. The first one is by Freeman [11] in 1958. In the following years other reports concerning this problem were published by various authors. The papers of Conti [6] and Vinokur [20] give a good overview of the technique used to analyze this kind of flow and give hints to other authors. We are interested in a mathematical analysis of this problem and reduce the necessary assumptions to a minimum. Especially, we do not want to assume incompressibility near the stagnation point, as it was done by Désidéri [8], because this contradicts our computational evidence. We are lead to results concerning the shape of the boundary layer which differ from those given by Vinokur [20].

In Section 2 we describe the physical, geometrical and mathematical assumptions needed for the analysis along the stagnation streamline. In Section 3 we derive a one-dimensional free boundary value problem (BVP) from the Euler equations in the case of an inviscid, steady flow in two space dimensions. Using this representation of the equations along the stagnation point streamline, we can replace the

mathematical assumptions by more physically motivated ones. Subsequently, the BVP will be examined at the stagnation point in particular, and a rough estimation of the structure of the solution near the stagnation point is presented. The results obtained in the first part will be used to analyze the numerical solution of the two-dimensional problem.

2 Assumptions

To analyze the stagnation point we need several assumptions. These can be divided into three groups:

- physical,
- geometrical and
- mathematical assumptions.

In this paper we restrict ourself to the steady, two-dimensional, inviscid flow. Chemical nonequilibrium is taken into consideration. On the other hand, the flow shall be in thermal equilibrium. We assume the mixture of gases composed of N components to be thermally perfect, i.e.

$$p = \rho R T \sum_{i=1}^N Y_i / W_i \quad \text{with} \quad (1)$$

$$a) \quad Y_i = \frac{\rho_i}{\rho}, \quad b) \quad \rho = \sum_{i=1}^N \rho_i, \quad (2)$$

where ρ_i is the partial density of the i th species. The gas is not assumed to be calorically perfect, i.e.

$$\gamma = \frac{c_p}{c_v} \neq \text{const.} \quad \text{with} \quad (3)$$

$$\begin{aligned} a) \quad c_p &:= \sum_{i=1}^N Y_i c_p^i(T) \neq \text{const.}, & d) \quad c_p^i(T) &:= c_v^i(T) + R/W_i, \\ b) \quad c_v &:= \sum_{i=1}^N Y_i c_v^i(T) \neq \text{const.}, & c) \quad c_v^i(T) &:= \frac{d e_i(T)}{dT}. \end{aligned} \quad (4)$$

The total energy E consists of the internal and kinetic energy and the heat of formation Δh :

$$\begin{aligned} a) \quad E &= e + \frac{1}{2}(u^2 + v^2) + \Delta h \quad \text{with} \\ b) \quad e &= \sum_{i=1}^N Y_i e_i(T), \\ c) \quad \Delta h &= \sum_{i=1}^N Y_i h_i^0 \end{aligned} \quad (5)$$

Here we do not enter into a detailed description of the model of internal energy. It is irrelevant to the following examination. But we want to remark that the numerical calculations have been carried out with the model of Hansen (see [14]). Thus, the steady, two-dimensional Euler equations are given by the N species equations

$$\operatorname{div}(\rho_i u, \rho_i v) = s_i, \quad i = 1, \dots, N, \quad (6)$$

the two equations of momentum

$$\begin{aligned} a) \quad & \operatorname{div}(\rho u^2 + p, \rho uv) = 0, \\ b) \quad & \operatorname{div}(\rho uv, \rho v^2 + p) = 0, \end{aligned} \quad (7)$$

and the energy equation

$$\operatorname{div}(\rho u H, \rho v H) = 0. \quad (8)$$

Herein the total enthalpy is defined as

$$H = E + \frac{p}{\rho}. \quad (9)$$

Because of the conservation of mass we obtain

$$\sum_{i=1}^N s_i = 0. \quad (10)$$

The s_i are the chemical production rates describing the chemical nonequilibrium. They depend on the partial densities ρ_i and the temperature T :

$$s_i = s_i(\rho_1, \dots, \rho_N, T), \quad i = 1, \dots, N. \quad (11)$$

Summation of the species equations (6) and (2) yields the ordinary continuity equation

$$\operatorname{div}(\rho u, \rho v) = 0. \quad (12)$$

As boundary conditions at the surface of the body we request that the flow velocity has no component normal to the body. We assume throughout this article that the system of equations (6) – (9) has a solution satisfying these boundary conditions. We assume that the body is symmetric and the free stream flow is parallel to this axis (the x -axis in this article). Further we assume that the resulting flow is symmetric with respect to the x -axis. Hence scalar physical quantities, e.g. ρ , p , T , are even functions with respect to y . The same applies for the x -component of a vector. The y -component of a vector is necessarily an odd function and thus vanishes along the x -axis. A curve $\mathbf{K} : \mathbb{R} \rightarrow \mathbb{R}^2$ which is tangent the velocity vector in each point, i.e.

$$\frac{d\mathbf{K}(s)}{ds} = \begin{pmatrix} u(\mathbf{K}(s)) \\ v(\mathbf{K}(s)) \end{pmatrix}. \quad (13)$$

is called a streamline. Since $v(x, 0) = 0$ the x -axis is a streamline. Further we assume that the body surface has a tangent at the intersection $(x_s, 0)$ with the x -axis which, due to symmetry, is normal to the x -axis. Since we have assumed

that a symmetric solution which satisfies the boundary conditions exists $(x_s, 0)$ is a stagnation point and the x -axis is a stagnation streamline. This enables us to derive a one-dimensional free BVP along the stagnation point streamline in an easy way.

Besides the physical and geometrical assumptions we need some mathematical ones for the stagnation point analysis. Essentially, they affect the Euler equations in the stagnation point. Since this point is a singular one, (6) – (9) need not to be valid there any more. To which extend this is the case will be analyzed in detail later. Here we will not assume that the Euler equations can be continued in a continuously differentiable way to the stagnation point. Thus, gradients are allowed to be infinite. Instead we only demand that the physical quantities are continuous functions up to the stagnation point, i.e. that they are bounded. An infinite density corresponds to an infinite compression which is even in the physical sense not acceptable. To guarantee a unique solution we have to assume

Assumption 1

$$\lim_{x \rightarrow x_s^-} \left(\frac{\partial Y_i}{\partial x} u \right) \Big|_{(x,0)} \stackrel{!}{=} 0, \quad i = 1, \dots, N \quad \text{and} \quad \lim_{x \rightarrow x_s^-} \left(\frac{\partial \rho}{\partial x} u \right) \Big|_{(x,0)} \stackrel{!}{=} 0. \quad (14)$$

We will derive a free BVP from the Euler equations along the stagnation line. From the structure of the BVP it is easy to see that assuming monotone and bounded functions of the state variables in the neighborhood of the stagnation point implies (14). Clearly the reduction of the two-dimensional problem to the one-dimensional BVP can only be done by assuming some information concerning the shape of the body to be known. In this article this is done by assuming that the following function is known

$$\frac{\partial v}{\partial y} \Big|_{(x,0)} = v_y(x) \quad x \in [x_0, x_s]. \quad (15)$$

In Section 7 we shall see how $v_y(x)$ relates to the shape of the body. The numerical simulation of the steady Euler equations by a shock-capturing method yields an almost constant value for v_y for a Mach 25 flow (see Figure 2). The deviation from this value behind the shock can be explained by the smearing of the shock because of the shock-capturing method.

3 The free boundary value problem

We will now analyze in detail the Euler equations (6) – (9) along the symmetry axis between the shock and the stagnation point, i.e. $x \in [x_0, x_s]$, $y = 0$. The equations (12), (6) – (9) can be written as

$$\begin{aligned} a) \quad & \frac{\partial(\rho u)}{\partial x} + \frac{\partial(\rho v)}{\partial y} = 0, \\ b) \quad & \frac{\partial Y_i}{\partial x} \rho u + Y_i \frac{\partial \rho u}{\partial x} + \frac{\partial Y_i}{\partial y} \rho v + Y_i \frac{\partial \rho v}{\partial y} = s_i(\rho_1, \dots, \rho_N, T), \quad i = 1, \dots, N, \end{aligned}$$

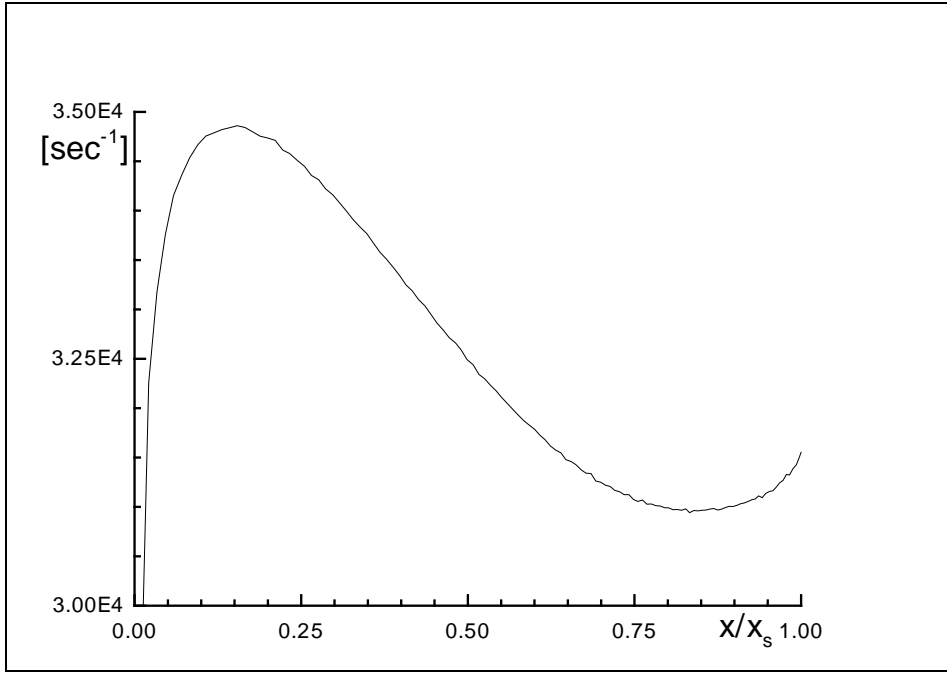


Figure 2: v_y along the stagnation streamline

$$c) \quad \frac{\partial(\rho u)}{\partial x} u + \rho u \frac{\partial u}{\partial x} + \frac{\partial p}{\partial x} + \frac{\partial(\rho u)}{\partial y} v + \rho u \frac{\partial v}{\partial y} = 0, \quad (16)$$

$$d) \quad \frac{\partial(\rho u)}{\partial x} v + \rho u \frac{\partial v}{\partial x} + \frac{\partial(\rho v)}{\partial y} v + \rho v \frac{\partial v}{\partial y} + \frac{\partial p}{\partial y} = 0,$$

$$e) \quad \frac{\partial(\rho u)}{\partial x} H + \rho u \frac{\partial H}{\partial x} + \frac{\partial(\rho v)}{\partial y} H + \rho v \frac{\partial H}{\partial y} = 0.$$

Notice that the partial densities ρ_i in (6) have been replaced by the mass fractions Y_i according to (2a). Putting (16a) in (16b-e) and using $v_y(x, 0) = 0$, these equations reduce to

$$\begin{aligned}
 b) \quad & \rho u \frac{\partial Y_i}{\partial x} + \rho v \frac{\partial Y_i}{\partial y} = s_i(\rho_1, \dots, \rho_N, T), \\
 c) \quad & \rho u \frac{\partial u}{\partial x} + \frac{\partial p}{\partial x} = 0, \\
 d) \quad & \rho u \frac{\partial v}{\partial x} + \rho v \frac{\partial v}{\partial y} + \frac{\partial p}{\partial y} = 0, \\
 e) \quad & \rho u \frac{\partial H}{\partial x} + \rho v \frac{\partial H}{\partial y} = 0.
 \end{aligned} \quad (17)$$

With the symmetry of the flow we get for $x \in [x_0, x_s]$, $y = 0$

$$a) \quad \frac{\partial \rho}{\partial x} u + \rho \frac{\partial u}{\partial x} = -\rho \frac{\partial v}{\partial y},$$

$$\begin{aligned}
b) \quad & \rho u \frac{\partial Y_i}{\partial x} = s_i(\rho_1, \dots, \rho_N, T), \quad i = 1, \dots, N, \\
c) \quad & \rho u \frac{\partial u}{\partial x} + \frac{\partial p}{\partial x} = 0, \\
d) \quad & \frac{\partial p}{\partial y} = 0, \\
e) \quad & \rho u \frac{\partial H}{\partial x} = 0.
\end{aligned} \tag{18}$$

(18d) gives no new equation because p is an even function in y . We further assume that the stagnation point $(x_s, 0)$ is the only point along the stagnation streamline where the velocity component u vanishes. Hence the last equation can be simplified to

$$e) \quad \frac{\partial H}{\partial x} = 0. \tag{19}$$

We now want to derive a system of equations for the quantities Y_i , u and p and their derivatives in x -direction. Therefore, the term $\partial\rho/\partial x$ in (18a) has to be replaced by the corresponding derivatives of Y_i , u and p . Therefore we solve (9) for p and replace E by (5) getting

$$p = \rho \left(H - \frac{u^2}{2} - \sum_{i=1}^N Y_i (e_i(T) + h^0) \right). \tag{20}$$

Differentiating this equation and taking (19e), (5) and (4c) into account, we obtain

$$\frac{\partial p}{\partial x} = \frac{\partial \rho}{\partial x} \left(H - \frac{u^2}{2} - \sum_{i=1}^N Y_i (e_i(T) + h^0) \right) + \rho \left(u \frac{\partial u}{\partial x} + \frac{\partial T}{\partial x} c_v + \sum_{i=1}^N \frac{\partial Y_i}{\partial x} (e_i(T) + h^0) \right). \tag{21}$$

Herein the term $\partial T/\partial x$ must also be substituted. By differentiating (1) we obtain

$$\frac{\partial p}{\partial x} = R\rho \frac{\partial T}{\partial x} \sum_{i=1}^N Y_i/W_i + RT \frac{\partial \rho}{\partial x} \sum_{i=1}^N Y_i/W_i + \rho RT \sum_{i=1}^N \frac{\partial Y_i}{\partial x} \frac{1}{W_i}. \tag{22}$$

We solve (22) for $\partial T/\partial x$ and replace it in (21):

$$\begin{aligned}
\frac{\partial \rho}{\partial x} \left(H - \frac{u^2}{2} - \sum_{i=1}^N Y_i (e_i(T) + h^0) + c_v T \right) = \\
\frac{\partial p}{\partial x} \left(1 + \frac{c_v}{R \sum_i \rho_i/W_i} \right) + \rho \sum_{i=1}^N \frac{\partial Y_i}{\partial x} \left(e_i(T) + H_i^0 - \frac{RT c_v}{W_i R \sum_j \rho_j/W_j} \right) + \rho u \frac{\partial u}{\partial x}
\end{aligned} \tag{23}$$

(3) and (4) yield

$$\frac{1}{\gamma - 1} = \frac{\sum_i Y_i c_v^i(T)}{R \sum_i Y_i/W_i}. \tag{24}$$

From this and (1) we obtain

$$c_v T = \frac{1}{\gamma - 1} \frac{p}{\rho}. \quad (25)$$

Together with (20) we get the equation

$$\frac{\gamma}{\gamma - 1} \frac{p}{\rho} \frac{\partial \rho}{\partial x} = \frac{\gamma}{\gamma - 1} \frac{\partial p}{\partial x} + \rho \sum_{i=1}^N \frac{\partial Y_i}{\partial x} \left(e_i(T) + h_i^0 - \frac{RT}{W_i(\gamma - 1)} \right) + \rho u \frac{\partial u}{\partial x}. \quad (26)$$

We introduce the frozen speed of sound

$$c_f^2 := \frac{\gamma p}{\rho}. \quad (27)$$

Thus, (26) simplifies to

$$\frac{\partial \rho}{\partial x} = \frac{\gamma}{c_f^2} \frac{\partial p}{\partial x} + \frac{\rho(\gamma - 1)}{c_f^2} \left(\sum_{i=1}^N \frac{\partial Y_i}{\partial x} \left(e_i(T) + h_i^0 - \frac{RT}{W_i(\gamma - 1)} \right) + u \frac{\partial u}{\partial x} \right)$$

and with (18b) we obtain

$$u \frac{\partial \rho}{\partial x} = u \frac{\gamma}{c_f^2} \frac{\partial p}{\partial x} + \frac{\gamma - 1}{c_f^2} \left(\sum_{i=1}^N s_i \left(e_i(T) + h_i^0 - \frac{RT}{W_i(\gamma - 1)} \right) + \rho u^2 \frac{\partial u}{\partial x} \right). \quad (28)$$

Putting this in equation (18a), we get

$$\frac{u}{p} \frac{\partial p}{\partial x} + \left(1 + (\gamma - 1) \frac{u^2}{c_f^2} \right) \frac{\partial u}{\partial x} = -v_y - \frac{\gamma - 1}{\gamma p} \sum_{i=1}^N s_i \left(e_i(T) + h_i^0 - \frac{RT}{W_i(\gamma - 1)} \right). \quad (29)$$

Because of (19e) we have

$$H(x, 0) = H(x_0, 0) =: H_0 = \text{const.}, \quad x \in [x_0, x_s], \quad (30)$$

and with (1), (5) and (9) we obtain an implicit equation for the temperature depending on Y_i and u :

$$f(Y_1, \dots, Y_N, u, T) := H_0 - \frac{u^2}{2} - \sum_{i=1}^N Y_i \left(e_i(T) + h_i^0 + RT/W_i \right) \stackrel{!}{=} 0. \quad (31)$$

According to (10) the chemical production rates s_i are linearly dependent. Assume the mixture of gases is composed of $m \leq N$ kinds of atoms. Then there exist m equations of balance

$$\sum_{i=1}^N a_{li} Y_i = c_l = \text{const.}, \quad l = 1, \dots, m \quad (32)$$

in the variables of mass fraction Y_i . By (18b) the linear dependence of the production rates follows immediately because

$$\sum_{i=1}^N a_{li} s_i = 0, \quad l = 1, \dots, m. \quad (33)$$

From the conservation of mass we get

$$\underbrace{\rho \frac{\partial u}{\partial x}}_{\text{bounded}} + u \frac{\partial \rho}{\partial x} = \underbrace{-\rho v_y}_{\text{bounded}}.$$

Thus, the term $u\partial\rho/\partial x$ is also bounded and as before continuous extendible to the stagnation point. Now we can expand u in a Taylor series

$$u(x) = u(x_s) + \frac{\partial u}{\partial x}(\xi)(x - x_s), \quad \xi \in (x, x_s).$$

We will show that the limit of $u\partial\rho/\partial x$ for x to x_s has to be zero. To do this, assume that $u\partial\rho/\partial x \neq 0$ in $[x_s - \varepsilon, x_s]$. If we assume that all the functions are monotone near the stagnation point and since $u\partial\rho/\partial x$ is continuous we obtain the estimate

$$0 < c_1 \leq \left| u \frac{\partial \rho}{\partial x} \right| \leq c_2$$

with some positive constants c_1 and c_2 for the whole interval $[x_s - \varepsilon, x_s]$, $\varepsilon > 0$. W.l.o.g. we assume $u\partial\rho/\partial x > 0$. Then we get

$$\begin{aligned} \frac{\partial \rho}{\partial x} &\geq c_1 \frac{1}{u} \\ &\geq c_1 \left(\frac{\partial u}{\partial x}(\xi)(x - x_s) \right)^{-1} \\ &\geq \frac{c_3}{(x_s - x)}. \end{aligned}$$

The last inequality holds since $|\partial u/\partial x| < c_4$ is bounded (see above). Integration of this inequality leads to an unbounded density which contradicts our assumption. This means that c_1 has to be zero and especially

$$\lim_{x \rightarrow x_s^-} u \frac{\partial \rho}{\partial x} = 0. \quad (37)$$

Then, from the same equation it follows that

$$\lim_{x \rightarrow x_s^-} \frac{\partial u}{\partial x}(x) = -v_y(x_s).$$

With the same analysis as above one obtains from

$$\rho u \frac{\partial Y_i}{\partial x} = s_i \quad \text{that} \quad s_i(x_s) = 0$$

at the stagnation point and so we have chemical equilibrium. This leads to

$$\lim_{x \rightarrow x_s} \rho u \frac{\partial Y_i}{\partial x} = 0. \quad (38)$$

We will summarize the above assumptions needed in the above derivation. We used

Assumption 2

- a) Y_i, ρ, u and p are bounded,
- b) all the bounded functions can be extended continuously to the stagnation point. This is obvious for the state variables u and p but also applies to the functions $\partial u/\partial x, \partial p/\partial x, u\partial\rho/\partial x$ and $\rho u\partial Y_i/\partial x$.
- c) Y_i, ρ and u are monotone in the neighborhood of the stagnation point, e.g. for each function f there exists a number $\varepsilon > 0$, so that for all $x, y \in [x_s - \varepsilon, x_s]$

$$\frac{\partial f}{\partial x}(x) \frac{\partial f}{\partial x}(y) \geq 0.$$

4 Existence of a solution

Now the question arises if a solution of the system of ordinary differential equations (34) with the algebraic conditions (2a), (32), (1) and (31) exists. This depends on the invertibility of the matrix \mathbf{A} . Before continuing we have to introduce the Mach number M defined by

$$M := \frac{\sqrt{u^2 + v^2}}{c_f}. \quad (39)$$

Using (34) yields

$$\det \mathbf{A} = (\rho u)^{N-m} (1 - M^2). \quad (40)$$

As mentioned in Section 1, the Mach number is strictly less than one (in the neighborhood of the stagnation point streamline). Consequently, the determinant of \mathbf{A} is zero if and only if $u(x, 0) = 0$ or one has a vacuum. So we have

$$\det \mathbf{A}(\mathbf{y}(x_s)) = 0. \quad (41)$$

This condition is satisfied only at the stagnation point, i.e. the system of differential equations can be transformed to

$$\dot{\mathbf{y}}(x) = \mathbf{A}^{-1}(\mathbf{y}(x)) \mathbf{b}(\mathbf{y}(x)) =: \mathbf{g}(\mathbf{y}(x)), \quad x \in [x_0, x_s], \quad \text{with} \quad (42)$$

$$g_i = \frac{s_{i+m}}{\rho u}, \quad i = 1, \dots, N - m, \quad g_{N-m+1} = \frac{\beta}{1 - M^2}, \quad g_{N-m+2} = -\rho u \frac{\beta}{1 - M^2}. \quad (43)$$

Because of the differentiability of the physical quantities along the stagnation point streamline, this is particularly valid for $\mathbf{g}(\mathbf{y}(x))$, $x \in [x_0, x_s]$. Thus (42) is solvable. The uniqueness follows from the initial values (35a) and the Lipschitz-continuity of \mathbf{g} (compare [21], p. 49 ff).

5 Determination of the initial values

To solve the differential-algebraic equations we have to determine the initial values (35a) behind the bow shock. Therefore we need the Rankine-Hugoniot condition for a scalar equation of the form

$$\frac{\partial w(x, y, t)}{\partial t} + \frac{\partial F(w(x, y, t))}{\partial x} + \frac{\partial G(w(x, y, t))}{\partial y} = 0 \quad \text{with} \quad (44)$$

$$F, G \in C^1(\mathbb{R}^2 \times \mathbb{R}^+, \mathbb{R}).$$

It can be derived in analogy to the one-dimensional case (compare [19], p. 246 ff). Consider the following situation. Assume $\Omega \subset \mathbb{R}^2 \times \mathbb{R}^+$ to be a connected domain

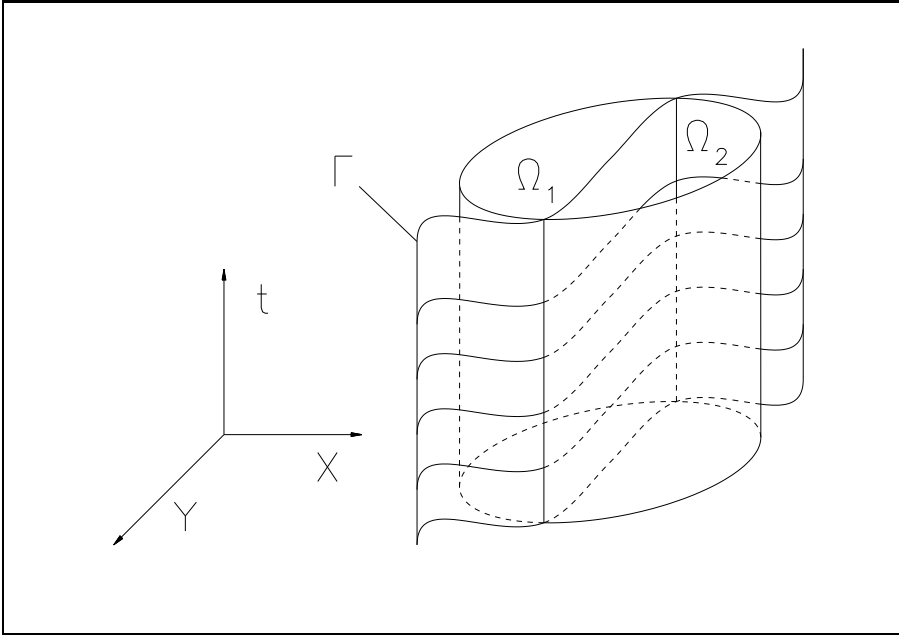


Figure 3: Discontinuity surface Γ

in space and time separated into two parts Ω_1 and Ω_2 by the discontinuity Γ . The solution w of (44) is constant in Ω_1 and Ω_2 and vanishes in $(\mathbb{R}^2 \times \mathbb{R}^+) \setminus \Omega$, i.e.

$$w|_{\Omega_i} \stackrel{!}{=} w_i = \text{const.}, \quad i = 1, 2, \quad w|_{(\mathbb{R}^2 \times \mathbb{R}^+) \setminus \Omega} = 0. \quad (45)$$

The surface Γ can be parameterized by the time t and the space parameter s as follows:

$$\mathbf{\Gamma}(t, s) := \begin{pmatrix} t \\ x(t, s) \\ y(t, s) \end{pmatrix} \quad (46)$$

In each point the tangential plane to Γ is spanned by the two vectors

$$\mathbf{\Gamma}_t := \frac{d\mathbf{\Gamma}}{dt} = \begin{pmatrix} 1 \\ x_t \\ y_t \end{pmatrix}, \quad \mathbf{\Gamma}_s := \frac{d\mathbf{\Gamma}}{ds} = \begin{pmatrix} 0 \\ x_s \\ y_s \end{pmatrix}. \quad (47)$$

The normal to Γ is defined by the vector product of $\mathbf{\Gamma}_t$ and $\mathbf{\Gamma}_s$

$$\mathbf{N} := \mathbf{\Gamma}_t \wedge \mathbf{\Gamma}_s = (x_t y_s - x_s y_t) \mathbf{e}_1 - y_s \mathbf{e}_2 + x_s \mathbf{e}_3.$$

Now the question arises how to choose w_1 and w_2 so that they form a weak solution (compare [19], p. 246 ff) of (44). Therefore we integrate over Ω :

$$\int_{\Omega} \operatorname{div}(w, F(w), G(w)) d\Omega dt = 0$$

Since $\Omega = \Omega_1 \cup \Omega_2$, this equation is equivalent to

$$\sum_{i=1}^2 \int_{\Omega_i} \operatorname{div}(w, F(w), G(w)) d\Omega dt = 0.$$

Using Gauss' theorem, the volume integral can be replaced by the surface integral

$$\sum_{i=1}^2 \int_{\partial\Omega_i} (w, F(w), G(w)) \tilde{\mathbf{N}}(t, s) ds dt = 0.$$

Here $\tilde{\mathbf{N}}$ is the outer normal to Ω_i . Because of (45) only the surface integral over Γ remains:

$$\sum_{i=1}^2 \int_{\Gamma} (w_i, F(w_i), G(w_i)) \mathbf{N}(t, s) (-1)^i ds dt = 0$$

Γ is arbitrary. Thus the Rankine-Hugoniot condition

$$(w_1 - w_2, F(w_1) - F(w_2), G(w_1) - G(w_2)) \mathbf{N} \stackrel{!}{=} 0 \quad (48)$$

holds. This is the jump condition for unsteady, two-dimensional hyperbolic conservation laws. The same equation is valid for systems. In this paper we are only interested in the steady equation. Then the jump condition becomes

$$(\mathbf{U}_1 - \mathbf{U}_2, \mathbf{F}(\mathbf{U}_1) - \mathbf{F}(\mathbf{U}_2), \mathbf{G}(\mathbf{U}_1) - \mathbf{G}(\mathbf{U}_2)) \begin{pmatrix} 0 \\ -y_s \\ x_s \end{pmatrix} \stackrel{!}{=} 0. \quad (49)$$

To determine the initial values (35a) at the point $(x, y) = (x_0, 0)$ we have to solve the jump condition (49). Due to the symmetry the normal is given by

$$\mathbf{N} = \begin{pmatrix} 0 \\ -1 \\ 0 \end{pmatrix}.$$

Then (49) yields

$$\mathbf{F}(\mathbf{U}_1) \stackrel{!}{=} \mathbf{F}(\mathbf{U}_2). \quad (50)$$

The fluxes \mathbf{F} and \mathbf{G} are given by (6) – (8) as

$$\begin{aligned} \mathbf{F}(\mathbf{U}) &= (\rho_1 u, \dots, \rho_N u, \rho u^2 + p, \rho uv, \rho u H)^T, \\ \mathbf{G}(\mathbf{U}) &= (\rho_1 v, \dots, \rho_N v, \rho uv, \rho v^2 + p, \rho v H)^T. \end{aligned} \quad (51)$$

In [1], p. 392 ff it is described how to solve (50), (51) iteratively. Therefore these equations are transformed into

$$\begin{aligned} a) \quad & Y_{i,2} = Y_{i,1}, \quad i = 1, \dots, N, \\ b) \quad & u_2 = u_1 \frac{\rho_1}{\rho_2}, \\ c) \quad & p_2 = p_1 + \rho_1 u_1^2 \left(1 - \frac{\rho_1}{\rho_2}\right), \\ d) \quad & v_2 = v_1, \\ e) \quad & e_2 = e_1 + \left(\frac{p_1}{\rho_1} - \frac{\rho_1}{\rho_2} u_1^2\right) \left(1 - \frac{\rho_1}{\rho_2}\right) + \frac{u_1^2}{2} \left(1 - \left(\frac{\rho_1}{\rho_2}\right)^2\right). \end{aligned} \quad (52)$$

The mass fractions $Y_{i,2}$ and the normal velocity v_2 are known because of (52a,d). Thus, only three equations remain for the four unknowns ρ_2, u_2, p_2, e_2 . The equation of state (1) and (5b) provide the additional condition

$$\begin{aligned} f) \quad & T = T(e, Y_1, \dots, Y_N), \\ g) \quad & \rho = \rho(p, T, Y_1, \dots, Y_N) = p \left/ \left(RT \sum_{i=1}^N \frac{Y_i}{W_i} \right) \right. . \end{aligned} \quad (52)$$

Now the equations (50b,c,e) can be solved iteratively by introducing $g := \rho_1/\rho_2$:

- 1) Set $g_0 := 0.1$ and $i = 0$.
- 2) Calculate $p_2^{(i)}$ and $\rho_2^{(i)}$ by (52c,e).
- 3) First calculate $T_2^{(i)}$, then $\rho_2^{(i)}$ with (52f,g).
- 4) Set $g_{i+1} := \rho_1/\rho_2^{(i)}$ and repeat step 2 – 4 until convergence.
- 5) Set $\rho_2 = g_{i+1}\rho_1$ and $u_2 = g_{i+1}u_1$.

Choosing the free-stream conditions for State 1, we can determine the initial values \mathbf{y}_0 .

6 Stagnation point analysis

In Section 4 we proved that there exists a unique solution \mathbf{y}_A of the initial value problem (34), respectively (42) and (35a). If there exists a point satisfying the condition (35b), \mathbf{y}_A is also the solution to the free BVP. \mathbf{y}_A is not known explicitly and therefore the existence of a finite point x_s satisfying (35b) cannot be proved mathematically. However we have shown that one has chemical equilibrium if u is 0.

We assume now, motivated by the physical boundary conditions for the 2D Euler equations (6) - (8), that there is a finite x_s which satisfies

$$u(x_s, 0) = 0. \quad (53)$$

At the stagnation point x_s the rank of \mathbf{A} is reduced to 2. Hence, the solution of (34) only exists in the half-open interval $[x_0, x_s)$. In the limit as x goes to x_s we shall need $N - m$ algebraic equations. The resulting system is a so-called differential-algebraic equation where the index is zero for $x < x_s$ and positive for $x = x_s$. To show this, we apply the local technique of Kunkel and Mehrmann (compare [15], [16]) to analyze the stagnation point. Therefore, the problem (34) is linearized:

$$\begin{aligned} \tilde{\mathbf{f}}(\mathbf{y}(x), \dot{\mathbf{y}}(x)) &:= \mathbf{A}_s \dot{\mathbf{y}}(x) + \mathbf{E}_s \mathbf{y}(x) = 0 \quad \text{with} \\ \mathbf{A}_s &:= \mathbf{A}(\mathbf{y}(x_s)), \quad \mathbf{E}_s := - \left. \frac{\partial \mathbf{b}(\mathbf{y}(x))}{\partial \mathbf{y}} \right|_{x=x_s} = - \begin{pmatrix} \mathbf{E}_{11} & \mathbf{E}_{12} \\ \mathbf{E}_{21} & \mathbf{E}_{22} \end{pmatrix}, \\ \mathbf{E}_{11} &:= \begin{pmatrix} \frac{\partial s_{m+1}}{\partial Y_{m+1}} & \cdots & \frac{\partial s_{m+1}}{\partial Y_N} \\ \vdots & & \vdots \\ \frac{\partial s_N}{\partial Y_{m+1}} & \cdots & \frac{\partial s_N}{\partial Y_N} \end{pmatrix}, \quad \mathbf{E}_{12} := \begin{pmatrix} \frac{\partial s_{m+1}}{\partial u} & \frac{\partial s_{m+1}}{\partial p} \\ \vdots & \vdots \\ \frac{\partial s_N}{\partial u} & \frac{\partial s_N}{\partial p} \end{pmatrix}, \\ \mathbf{E}_{21} &:= \begin{pmatrix} \frac{\partial \beta}{\partial Y_{m+1}} & \cdots & \frac{\partial \beta}{\partial Y_N} \\ 0 & \cdots & 0 \end{pmatrix}, \quad \mathbf{E}_{22} := \begin{pmatrix} \frac{\partial \beta}{\partial u} & \frac{\partial \beta}{\partial p} \\ 0 & 0 \end{pmatrix}. \end{aligned} \quad (54)$$

This can be derived from (34) as follows. First, the problem is written as

$$\mathbf{f}(\mathbf{y}, \dot{\mathbf{y}}) := \mathbf{A}(\mathbf{y}) \dot{\mathbf{y}} - \mathbf{b}(\mathbf{y}) = 0.$$

Then the total derivative of \mathbf{f} is given by

$$d\mathbf{f} = \left(\frac{\partial \mathbf{A}}{\partial \mathbf{y}} \dot{\mathbf{y}} - \frac{\partial \mathbf{b}}{\partial \mathbf{y}} \right) d\mathbf{y} + \mathbf{A} d\dot{\mathbf{y}} = 0.$$

Assuming \mathbf{A} and $\partial \mathbf{b} / \partial \mathbf{y}$ to be locally constant – e.g. at the stagnation point – we get

$$d\tilde{\mathbf{f}} = \mathbf{A}_s d\dot{\mathbf{y}} - \mathbf{E}_s d\mathbf{y}.$$

This is the total derivative of $\tilde{\mathbf{f}}$ (compare (54)) and therefore zero, too. Now we determine the singular value decomposition of \mathbf{A}_s :

$$\mathbf{U}^T \mathbf{A}_s \mathbf{V} = \Sigma \quad \text{with}$$

$$\mathbf{U}^T := \begin{pmatrix} & \mathbf{I}_2 \\ \mathbf{I}_{N-m} & \end{pmatrix}, \quad \mathbf{V} := \begin{pmatrix} & \mathbf{I}_{N-m} \\ \mathbf{I}_2 & \end{pmatrix}, \quad \mathbf{\Sigma} := \begin{pmatrix} \mathbf{I}_2 & & & \\ & 0 & & \\ & & \ddots & \\ & & & 0 \end{pmatrix}.$$

Here I_k is the identity matrix in $\mathbb{R}^{k \times k}$. Then the product

$$\mathbf{U}^T \mathbf{E}_s \mathbf{V} = \begin{pmatrix} \mathbf{E}_{22} & \mathbf{E}_{21} \\ \mathbf{E}_{12} & \mathbf{E}_{11} \end{pmatrix}$$

is formed. Applying Theorem 4.13 of [15], the following characterization of the linear problem (54) can be shown:

$$\text{Index 1} \iff \det \mathbf{E}_{11} \neq 0$$

Because of this relation we get an index larger than one once we have shown that \mathbf{E}_{11} is singular. To show this observe that we have seen that the chemical reactions are in equilibrium at the stagnation point. We also know that the total entropy S is constant for an equilibrium flow. Hence we have an additional equation which relates the mass fractions in the same manner as the equations of balance did before. Consequently, at least one eigenvalue has to approach zero. This means that the matrix \mathbf{E}_{11} is singular. If we would use the perturbation index of a DAE introduced in [13] again we would observe an increase of the index at x_s to a number larger than one. With this definition the regularity of the matrix \mathbf{E}_{11} leads to an estimation of the error of the solution for small disturbances. Nevertheless, for given u and p we can solve the equations

$$s_l(Y_{m+1}, \dots, Y_N, u, p) = 0, \quad l = m + 1, \dots, N$$

for Y_j , and from this we are able to solve the system, as we will see later. To sum up, this kind of equations do not fit into the standard definitions of the index of a DAE.

We now consider the system (34) in the limiting case for x to x_s . Most of the work is done in Section 3 and we will summarize the results. We know that $\partial u / \partial x$ and $\partial p / \partial x$ are bounded and for the limit $x \rightarrow x_s$

$$\lim_{x \rightarrow x_s} \frac{\partial u}{\partial x}(x) = -v_y(x_s) \quad \text{and} \quad \lim_{x \rightarrow x_s} \frac{\partial p}{\partial x}(x) = 0$$

holds so that the pressure and velocity functions are smooth up to x_s . This is the reason why we have chosen these variables for the BVP in (34). On the other hand the equations (37) and (38)

$$\lim_{x \rightarrow x_s} u \frac{\partial \rho}{\partial x}(x) = 0 \quad \text{and} \quad \lim_{x \rightarrow x_s} \rho u \frac{\partial Y_i}{\partial x}(x) = 0$$

allow infinite gradients for the mass fractions Y_i and the density ρ at the stagnation point. The last of these equation forces the chemical reactions to some equilibrium state at this point.

As we have seen by the example in Figure 2 we can assume that $\partial v(x, 0)/\partial x$ is smooth or even constant. Since u and p are smooth functions, the equations (18c) and (29) can be used to obtain a solution for $u(x, 0)$ and $p(x, 0)$ in a numerically stable way. We still need $N - m$ additional equations for the mass fractions Y_i , $i = m + 1, \dots, N$. Due to the chemical equilibrium we get these equations from the chemical production rates s_i . For given u and p , obtained from the differential equations, we can solve the $N - m$ equations of chemical equilibrium for the unknown mass fractions Y_i , $i = m + 1, \dots, N$. At the stagnation point this implies that the regular problem (34) becomes a so-called higher index problem as mentioned above (compare [12], [4]). Higher index problems can be treated numerically, e.g. by backward-differencing methods, but we are not aware of any results concerning differential-algebraic equations with changing index. As will be described in more detail in Section 7, we have solved the initial value problems (34), (35a) with the DASSL-code [4] until $u(x)$ becomes zero, see Table 1. For large bodies, i.e. $v_y(x, 0)$ is constant and small, the results at the stagnation point are almost equivalent to the correct ones obtained from equilibrium chemistry using $u = 0$ and $p_s = \lim_{x \rightarrow x_s} p$, see Table 2.

Let us now describe how one obtains these correct results using analytical properties. Since by (36) $\partial p/\partial x = 0$ at the stagnation point, we set p_s to the last value of p computed before reaching the point where \mathbf{A} becomes singular. The m equations of balance in (32) have a very simple form so that one can choose $N - m$ parameters Y_j and express the remaining Y_k in terms Y_j . For simplicity we change the enumeration so that the first m mass fractions are functions of the last $N - m$ as we did before. From the fact that the temperature can be expressed as a function of the mass fractions Y_i only, since $u = 0$, we can express the density

$$\rho = \rho(Y_{m+1}, \dots, Y_N, p) = p \left/ \left(RT(Y_{m+1}, \dots, Y_N) \sum_{i=1}^N \frac{Y_i}{W_i} \right) \right. \quad (55)$$

as a function of the last $N - m$ mass fractions Y_j and the pressure p . We now take $N - m$ linearly independent reaction rates s_j and calculate the root for the given pressure by some iterative method (e.g. Newton's). With the independent mass fractions we then compute the remaining thermodynamical quantities at the stagnation point.

Finally we would like to show that the stagnation point values do depend on the shape and size of the body. To do this, we observe that given the pressure p_s one can compute Y_i, ρ and T using $u = 0$ and equations which do not involve v_y . In principle one can write $T = T(p_s)$ and the functional relation $T(\cdot)$ is independent of v_y . From experiments we see that p_s does depend on v_y and hence T depends on v_y since obviously $\partial T/\partial p \neq 0$. The same is of course true for the other variables Y_i and ρ . We have given the values for some v_y in Table 2.

It was pointed out in the 1960s by Conti [5] and other authors and became a new topic during the Antibes workshops in 1990 and 1991 that the nonequilibrium flow past a blunt body may generate a chemical boundary layer for small bodies (see

the discussion in Section 8 and figures). In all our investigations we chose our assumptions in a way to allow some kind of boundary layer, as long as the quantities stay bounded. We now want to get a rough idea of this boundary layer. We use the dependence on the smooth functions u and p . Hence (18b) becomes

$$Y' = \frac{1}{u\rho} S(Y, u, p)$$

where $Y = (Y_{m+1}, \dots, Y_N)^T$. At the stagnation point we have equilibrium chemistry. Then we can assume an expansion of the form

$$S(Y, u, p) = J(Y, u, p)(Y - Y^*) + O(\|Y - Y^*\|^2). \quad (56)$$

Let us further assume that there exists a regular matrix T independent of Y , u , p such that $TJT^{-1} = \Lambda$ is a real diagonal matrix with distinct eigenvalues. From some examples we know that the eigenvalues of J are real distinct. From this we have at least a smooth dependence of the eigenvectors on the variables Y . If we omit the higher order terms in (56), we obtain for the new variable $Z = T(Y - Y^*)$ a system of $N - m$ independent ordinary differential equations

$$Z' = \frac{1}{u\rho} \Lambda(u, p)Z, \quad Z(x_s) = 0. \quad (57)$$

Expanding the solution around x_s and using $u = v_y(x_s - x)$ gives for each component z_i

$$z_i(x) = c_s(x_s - x)^{-\frac{\lambda_i}{v_{ys}\rho_s}} \quad (58)$$

where λ_i is the i -th eigenvalue of J , ρ_s is the density at the stagnation point and v_{ys} is $v_y(x_s)$. Observe that the eigenvalues λ_i are negative. One sees that there is a boundary layer if there is an eigenvalue λ_i with $-\lambda_i < v_{ys}\rho_s$. Moreover, the layer becomes thinner if v_{ys} is increasing.

If the reactions become infinitely fast, i. e. $-\lambda_i$ tends to infinity, then one does not have a boundary layer and in fact one has a flow with equilibrium chemistry. One knows from the results in both Antibes workshops that today's schemes have no problem computing equilibrium Euler flow, i. e. one obtains the correct stagnation point temperature. In order to set (58) in the proper perspective let us briefly discuss a particular example. In Figure 12 we plot λ_i/ρ along the stagnation streamline in the case of a circular body with the five species chemistry model described later. Since one has conservation of the total number of the N and O atoms, two eigenvalues are identically zero. Directly behind the shock two eigenvalues are complex and we have indicated only $|\lambda_i|/\rho$. Further downstream this pair of conjugate complex eigenvalues becomes two real eigenvalues and λ_i/ρ is approximately $-1.03 \mu\text{sec}^{-1}$ and $-0.33 \mu\text{sec}^{-1}$ at the stagnation point. Since $v_y \sim 0.0327 \mu\text{sec}^{-1}$, these two eigenvalues do not give rise to a boundary layer. However, the third eigenvalue λ_3 does. If we use the value of $\lambda_3/\rho \sim 0.01 \mu\text{sec}^{-1}$ which occurs just before the stagnation point, we obtain an exponent of 0.3 in (58). Note that in 2D calculations we get estimates of approximately 0.4 for this exponent.

However from Figure 12 we see that the eigenvalue λ_3 becomes zero at the stagnation point, a fact which contradicts our assumption. Hence one has to improve the above analysis. There are indications that the singularity is stronger than of the type $(x_s - x)^\alpha$. In this case we will use the ansatz

$$\lambda_3 = \frac{a}{\ln(b(x_s - x))}$$

for the eigenvalues approaching zero. The choice of $(x_s - x)^\alpha$ leads to no solution. Then we obtain for the corresponding variables z_3 from (57)

$$z_3' = \frac{1}{v_y(x_s - x)} \frac{a}{\ln(b(x_s - x))} z_3.$$

This equation can be integrated, and we obtain a solution for z as

$$z_3(x) = \left(-\frac{c}{\ln(d(x_s - x))} \right)^e$$

with the integration constants c , d and e . Differentiating with respect to x , we can calculate the constants from

$$-\frac{e}{\ln(d(x_s - x))} \frac{d}{d(x_s - x)} = -\frac{1}{v_y(x_s - x)} \frac{a}{\ln(b(x_s - x))}$$

and get that

$$a = e v_y \quad \text{and} \quad b = d.$$

It was surprising how good this simple ansatz corresponds to the function calculated in the examples. To show this, we assumed $e = 2$ and plotted in Figure 13 the function

$$\exp(2v_y/\lambda_i(x))$$

which is the inverse function to $1/\ln(x)$. This function is nearly a straight line in the neighborhood of the stagnation point, and from this we know that in this special example the exponent of the first term in an expansion of the solution near the stagnation point is two and $b = 62.3$.

Let us briefly relate the present analysis to earlier investigations. Conti [6] and Vinokur [20] give good surveys over earlier work on analyzing chemical boundary layers. Conti uses in [5] and in more detail in [6] the method of successive truncations. The idea is that one expands unknown functions with respect to powers of $\sin\theta$ and $\cos\theta$, where θ is the angle in polar coordinates. This leads to a sequence of systems of ordinary differential equations. However, each system requires knowledge of at least one unknown which originates from the next system. This is similar to our v_y function. While in our analysis v_y is taken from a 2D computation and incorporates the geometry of the body as the needed additional function, Conti [6] uses the bow shock radius r_s as a geometrical parameter and truncates the expansion of the pressure after one term. To get more accurate results one solves successively several of these systems of ordinary differential equations. In Vinokur [20] the chemical

boundary layers are shown to exist using a local analysis at the stagnation point similar to the derivation we proposed to obtain the necessary condition $-\lambda_i < v_{ys}\rho_s$ for existence of a boundary layer. The basic behavior of the boundary layer given by Vinokur is $(x_s - x)^\alpha \log^\beta(x_s - x)$, $\beta \in \{0, \dots, N - m\}$. We have shown above that this cannot be correct if an eigenvalue goes to zero. Moreover it seems that our method to compute the standoff distance x_s using v_y is new. Finally we want to mention that in [8] the existence of a possible chemical boundary is pointed out, but the assumption of incompressibility at the stagnation point contradicts our results, see Figure 1.

7 Parameter study

As mentioned in Section 2 we are losing all information of the geometry by passing from the 2D Euler equations to the one-dimensional BVP on the stagnation point streamline. The information is made available by the function $v_y(x)$. The shape of this function is not known a priori. Because of the information from Figure 2 we now assume $v_y = \text{const}$. We want to examine the influence of this quantity on the solution of the BVP. Therefore we use the 5-component model of air by Park (compare [17]), consisting of N , N_2 , O , O_2 and NO . The free-stream conditions are

$$\begin{aligned} p_\infty &= 2.53 \text{ Pa}, \\ \rho_\infty &= 4.15 \times 10^{-5} \text{ kg/m}^3, \\ T_\infty &= 211 \text{ K}, \\ M_\infty &= 25, \\ Y_{N_2, \infty} &= 0.79, \\ Y_{O_2, \infty} &= 0.21, \\ Y_{O, \infty} &= Y_{N, \infty} = Y_{NO, \infty} = 0. \end{aligned}$$

With that we calculate the initial values by the jump condition (50) getting

$$\begin{aligned} p_0 &= 1935 \text{ Pa}, \\ \rho_0 &= 3.27 \times 10^{-4} \text{ kg/m}^3, \\ T_0 &= 20485 \text{ K}, \\ M_0 &= 0.34, \\ Y_{i, 0} &= Y_{i, \infty}. \end{aligned}$$

To solve the system of differential equations (34) we use the DASSL-solver [4]. The parameter v_y varies over the values 100, 1000, 10000 and 100000. In Figures 4 – 8 several quantities are plotted along the stagnation point streamline which is scaled by the stand-off distance. Table 1 shows the quantities at the stagnation point obtained with this solver. The results in Table 2 are the roots of the reaction rates for N_2 , O_2 and NO using the chemical equilibrium and the procedure described at the end of Section 6. The value $v_y = 32714 \text{ sec}^{-1}$ is added because of the comparison with the 2D calculation. Two points are especially noticeable:

- 1) Near the stagnation point a “chemical layer” is formed for large v_y where the temperature strongly decreases and the density increases accordingly at almost constant pressure (36).
- 2) The stand-off distance is increasing with decreasing v_y .

The chemical layer is too thin to give a physical explanation for it. The thickness is approximately $10^{-12} m$ and hence it is several orders of magnitudes smaller than the diameter of the molecules. Nevertheless, a numerical scheme should give the correct solution to show that the physical model is wrong. The question arises whether the layer can be realized by a two-dimensional numerical scheme. Then the cell diameter near the body has to be much smaller than the thickness of the layer. Let us assume that we would only need 10 cells to resolve the boundary layer. Hence the smallest cell would have to be of size $10^{-13} m$. The finest cell used in our calculations is $10^{-4} m$. Hence we are still off by a factor of 10^9 . In Section 8 we present a method how to get a better approximation of the information in the layer by a two-dimensional scheme using coarse grids.

Let us now explain the relation of the stand-off distance and the parameter v_y . To do this, we integrate the equation of continuity (18a) along the stagnation point streamline. This yields

$$\int_{x_0}^{x_s} \frac{\partial \rho u}{\partial x} \Big|_{(x,0)} dx + \int_{x_0}^{x_s} v_y(x) \rho(x,0) dx = 0.$$

Using (53) and the mean value theorem of integral calculus we obtain

$$-\rho u|_{(x_0,0)} + v_y(\xi) \rho(\xi,0) (x_s - x_0) = 0.$$

Herein ξ is an intermediate point of the interval (x_0, x_s) . The stand-off distance is then given by

$$|x_s - x_0| = \frac{1}{v_y(\xi)} \frac{\rho_0 u_0}{\rho(\xi,0)}. \quad (59)$$

This is the explanation to Point 2 of the numerical interpretation.

There still remains the question how to choose v_y . One possibility is given by the jump condition (49). We assume that the bow shock at the intersection point of the symmetry axis can locally be described by a circle of radius R_0 . The jump condition for an oblique shock (see (48) and [2]) gives the following relation between v_y and R_0 :

$$v_y = \frac{2u_\infty}{(\gamma + 1)R_0} \quad (60)$$

A similar consideration can be made at the body. This has been carried out in [2], p. 250 ff. Incompressibility and a pressure distribution according to Newton’s theory has been assumed. This gives

$$v_y \approx \frac{1}{R_s} \sqrt{\frac{2(p_s - p_\infty)}{\rho_s}} \quad (61)$$

where R_s is the local radius of the body at the stagnation point. There exist at least two references ([3], [18]) where the radii R_0 and R_s are quantitatively related. Billig [3] fits a curve by experimental data and Probst/Hayes [18] derive an asymptotic expansion with respect to the term ρ_∞/ρ . The formulas (60) and (61) imply the linearity between the radius of the body at the stagnation point and the stand-off distance. Thus we have

$$\begin{aligned} v_y \rightarrow 0 &\Leftrightarrow R_s \rightarrow \infty \Leftrightarrow x_s - x_0 \rightarrow \infty, \\ v_y \rightarrow \infty &\Leftrightarrow R_s \rightarrow 0 \Leftrightarrow x_s - x_0 \rightarrow 0. \end{aligned} \tag{62}$$

For the problem under consideration we calculated

$$\begin{aligned} p_s &= 2061 \text{ Pa}, \\ \rho_s &= 6.5 \times 10^{-4} \text{ kg/m}^3. \end{aligned}$$

With (61) and $R_s = 0.1$ this yields

$$v_y = 25161 \text{ sec}^{-1}.$$

Using the estimation of the shock radius

$$R_0 = 1.386 R_s \exp\left(1.8/(M_\infty - 1)^{0.75}\right)$$

according to Billig [3] in (60) we obtain alternatively

$$v_y = 37200 \text{ sec}^{-1}.$$

Figure 2 shows the quantity v_y calculated by a two-dimensional Euler computation. The value of v_y is about 32500 sec^{-1} . Using this value for the solution of (34) we calculated the same stand-off distance

$$|x_0 - x_s| = 0.02075 \text{ m}$$

as for the 2D Euler equations. According to (60) this corresponds to a bow shock radius of 0.196 m . Thus the formula (61) cannot be used for an a-priori estimate of v_y . Moreover, the radius R_0 depends nonlinearly on the radius R_s . The assumptions made for existing formulas to estimate the stand-off distance and the curvature of the bow shock are not satisfied in a hypersonic flow with chemical nonequilibrium. Here the estimated values differ by more than 30%. Because v_y is not known a priori, the stand-off distance can only be determined by a two-dimensional calculation. Vice versa the numerical 2D solution can be verified quantitatively at critical points. In contrast to shock-capturing schemes, there exist an error analysis and quantitative statements for the solution of ordinary differential equations. Thus we developed an alternative validation method besides experimental data, especially when some physical phenomena are absent, as it is the case with Euler flow.

8 Numerical analysis

The previous investigations provided a good approximation of the solution along the stagnation point streamline. For values $v_y > 1000$ the figures in the appendix show a thin chemical boundary layer near the body surface. We use this information in our 2D calculations to obtain better results. The question arises how a finite volume method can describe such a behavior. Obviously, a boundary layer which is less than 10^{-12} m thick cannot be resolved by volumes with a diameter which is eight orders of magnitude larger.

We want to investigate if there is any layer and what happens in the limit when the grid size goes to zero. Therefore we extrapolate the values on the stagnation point streamline in the flow field to the body surface. We use the same ansatz

$$y(x) = y_s + c(x_s - x)^\alpha \quad (63)$$

as in (58). The parameters y_s , c and α can be either fitted using the three nearest points or calculated from a nonlinear least square problem to reduce the influence of the errors due to boundary conditions. Both methods give almost the same results. In the tables the results of the least square method are shown.

The most interesting and sensitive variable is the temperature. There are three possibilities to calculate this temperature. First, we extrapolate the temperature directly. This value is given in line eight of the tables in the appendix and called T . Secondly, we extrapolate the conserved quantities ρ_1, \dots, ρ_N and ρE and set $u = v = 0$. With (5) we then calculate the temperature (called $T_{\rho E}$). The gradient of the energy may also be infinite. From (36) we know that the pressure gradient is zero in x_s . Thirdly, we take the pressure in front of the wall, the extrapolated partial densities and use (1) to calculate the temperature T_p .

For this investigation we have done six test calculations for a flow past a cylinder of radius 0.1 m. The grid size varies from 0.5 mm to 0.1 mm in steps of 0.1 mm. The numerical method used is a modified van Leer flux-vector-splitting completely described in [9]. The Tables 3 – 7 show the results of the extrapolation. The quantity y_s is the value at the wall. The exponent α reflects the behavior of the function. If α is greater than one, the function is smooth with a bounded gradient at the stagnation point. If α is less than one, we have a root function with an infinite gradient at x_s . From the value of α we can also estimate the thickness of the boundary layer. The smaller α gets, the thinner the boundary layer becomes. In Tables 3 – 7 all the quantities change monotonously when refining the mesh. The exponents of energy, temperature and partial density of nitrogen atoms decrease whereas the exponent of nitrogen molecules increases and is greater than one. We find that with decreasing mesh size the boundary layer is more and more resolved. Even in the case of the coarse mesh we can reduce the temperature by 350 K to 8159 K. On the finest mesh we get 7780 K. The temperature T_p is always higher than $T_{\rho E}$. Moving to the finer grid, the value of the pressure increases to 2100 Pa, but $p_{\rho E}$ using the temperature $T_{\rho E}$ and (1) decreases to 2074 Pa. The corresponding value obtained from the BVP is 2061 Pa.

For comparison we used the standard van Leer method on the finest grid with step-size 0.1 mm . The extrapolated values are shown in Table 8. All the exponents α are greater than one even for density and temperature. So the solution of this 2D calculation suggests a smooth continuation to the stagnation point. The extrapolation (63) is not useful here. The extrapolated values in Table 3 of the coarse grid are better than in Table 8 for the fine grid.

9 Final remarks

In the Sections 2 and 3 we transformed the compressible Euler equation into a free BVP. A symmetric flow is only assumed for simplicity. This transformation is also possible for an arbitrary geometry. In this case we first transform the Cartesian coordinate system into one consisting of streamlines and their normals. Then the equations get the same structure used in the Sections 2 and 3.

The mathematical assumptions (14) are implied by the more obvious ones in Assumption 2 and they are valid for nearly all interesting initial conditions. In the case of the Euler equations and for the special chemical model we are able to compute all the values up to the stagnation point. So we have the possibility to investigate this point in detail without any assumption of incompressibility as in [1] or [8]. From Figure 9 it is clear that especially this assumption is violated.

In Section 6 we showed that a unique solution on the stagnation streamline exists, even when the matrix \mathbf{A} becomes singular. Nevertheless it is still complicated to calculate this solution numerically. The authors are not aware of any papers which deal with the numerical solution of DAE's with index jump. So we moved the problem from one class to another. The theory of DAE's gives us more powerful tools to analyze this problem than the theory of hyperbolic conservation laws does. Only the knowledge of all the analytical properties and the special problem enables us to obtain satisfactory results at the stagnation point (see Table 1 and 2). As mentioned in Section 8, we now can estimate the accuracy of a 2D Euler calculation. We can compare different Euler solvers and decide which one is more suitable for the problem. Such a comparison of two schemes in [9] shows that the standard van Leer scheme is not a good choice (see Fig. 11). The numerical diffusion is too high to resolve the structure generated by the chemical reactions. In contrast to this, the modified scheme gives good results. Using the extrapolation (63), the stagnation point temperature can be reduced.

A new interesting result is the behavior of the pressure. We noticed a difference between the solution of the BVP and the 2D calculation over the whole interval whereas the temperature only differs near the stagnation point. It would be interesting to know how the 3% pressure difference influences the stand-off distance. For example the pressure between an ideal gas flow and a chemical reacting one differs by only 15 – 20% but the stand-off distance is reduced to less than half. So the question of good boundary conditions arises and a more general extrapolation than

in (63) may be a good answer. In [10] a first attempt is made to construct new boundary conditions for this kind of flow.

Let us add some remarks concerning the physical relevance of these results. From the solution of (34) we obtain the size of the boundary layer to be less than 10^{-12} m. So it is smaller than the diameter of the atoms involved. Such a thin layer contradicts the fundamental continuum assumption. In every volume element (the physical, not the numerical ones), including those in the layer, there have to be enough particles so that this element can be regarded as a continuum; otherwise one has to use the Boltzmann equation. This assumption is strongly violated by the solution. Thus it is not reasonable to use analytical results such as chemical equilibrium as boundary conditions. Perhaps the numerical solution may be closer to the physical one than the analytical solution.

Notation

M	Mach number
u	velocity component in x-direction
v	velocity component in y-direction
p	pressure
ρ	density
ρ_i	partial density of species i
Y_i	mass fraction of species i
e_i	internal energy of species i
e	internal energy
$c_{v,i}$	specific heat capacity at constant volume of species i
c_v	specific heat capacity at constant volume
$c_{p,i}$	specific heat capacity at constant pressure of species i
c_p	specific heat capacity at constant pressure
γ	ratio of heat capacities
W_i	molar weight of species i
R	universal gas constant
T	temperature
c_f	frozen speed of sound
s_i	chemical reaction rate of species i
E	total energy per mass
H	total enthalpy per mass
N	number of species
h_i^0	heat of formation of species i
Δh	heat of formation
R_s	local radius of the body
R_0	local radius of the shock front
\mathbf{N}	outer normal
$\mathbf{\Gamma}$	shock surface

Acknowledgement

We want to thank Prof. Christian Lubich, ETH Zürich, and PD Dr. Volker Mehrmann, University of Bielefeld, for valuable discussions on DAE's and Prof. W.J. Beyn, University of Bielefeld for a discussion on singular problems. A large portion of this research has been performed under the contract: Hermes Program Phase C1, R + D ANE 19/87 step 3.

References

- [1] J. D. Anderson. *Modern Compressible Flow*. McGraw-Hill Book Company, 1982.
- [2] J. D. Anderson. *Hypersonic and High Temperature Gas Dynamics*. McGraw-Hill Book Company, 1989.
- [3] F. S. Billig. Shock wave shapes around spherical and cylindrical nosed bodies. *Jour. Spacecraft*, 1967.
- [4] K. E. Brenan, S. L. Campbell, and L. R. Petzold. *Numerical Solution of Initial Value Problems in Differential Algebraic Equations*. North Holland, 1989.
- [5] Raul J. Conti. Stagnation equilibrium layer in nonequilibrium blunt body flow. *AIAA J.*, 2:2044–2046, 1964.
- [6] Raul J. Conti. A theoretical study of non-equilibrium blunt body flow. *J. Fluid Mech.*, 24(1):65–88, 1966.
- [7] J.-A. Désidéri, R. Glowinski, and J. Périaux, editors. *Hypersonic Flows for Reentry Problems, Proceedings of the Workshop held in Antibes, France, 22-25 January, 1990*, volume 2. Springer Verlag, 1992.
- [8] Jean-Antoine Désidéri. Some comments on the numerical computations of reacting flows over the double-ellipse (double ellipsoid). In [7], volume 2, 1992.
- [9] Michael Fey and Rolf Jeltsch. Influence of numerical diffusion in high temperature flow. In I. L. Rhyming, editor, *Proceedings of the 9th GAMM Conference on Numerical Methods in Fluid Dynamics, Notes on Numerical Fluid Mechanics*. Vieweg Verlag, 1992.
- [10] Michael Fey, Rolf Jeltsch, and Peter Karmann. Special aspects of reacting inviscid blunt body flow. In J.-A. Désidéri, R. Glowinski, and J. Périaux, editors, *Hypersonic Flows for Reentry Problems, Proceedings of the Workshop held in Antibes, France, April, 1991*, volume 3. Springer Verlag, to appear.
- [11] N. C. Freeman. Non-equilibrium flow of an ideal dissociating gas. *J. Fluid Mech.*, 4:407, 1958.

- [12] E. Griepentrog and R. März. Differential–algebraic equations and their numerical treatment. *Teubner Texte zur Mathematik*, 1986.
- [13] Ernst Hairer, Christian Lubich, and Michel Roche. *The Numerical Solution of Differential-Algebraic Systems by Runge-Kutta Methods*. Number 1409 in Lecture Notes in Mathematics. Springer Verlag, 1989.
- [14] C. F. Hansen. Approximation for the thermodynamics and transport properties of high-temperature air. Technical Report TR-50, NASA, 1959.
- [15] P. Kunkel and V. Mehrmann. Smooth factorisations of matrix valued functions and their derivatives. *Numerische Mathematik*, 60:115–132, 1991.
- [16] P. Kunkel and V. Mehrmann. Canonical forms for linear differential-algebraic equations with variable coefficients. Technical Report 69, Inst. f. Geometrie u. Prakt. Mathematik, RWTH Aachen, 1992.
- [17] Chul Park. On convergence of computation of chemically reacting flows. Technical Report 085-0247, AIAA, 1985.
- [18] R. F. Probstein and W. D. Hayes. *Hypersonic Flow Theory*. Academic Press, 1966.
- [19] J. Smoller. *Shock Waves and Reaction–Diffusion Equations*. Springer Verlag, 1982.
- [20] Marcel Vinokur. On stagnation point conditions in non-equilibrium inviscid blunt body flows. *J. Fluid. Mech.*, 30:49–75, 1970.
- [21] W. Walter. *Gewöhnliche Differentialgleichungen*. Springer Verlag, 1976.

A Tables

Table 1: Solution at the stagnation point with DAE					
$v_y =$	100	1000	10000	32437	100000
Y_N	4.61868E-01	4.59821E-01	4.32618E-01	4.10828E-01	3.82207E-01
Y_{N_2}	3.27694E-01	3.29713E-01	3.56375E-01	3.77456E-01	4.04637E-01
Y_O	2.09494E-01	2.09461E-01	2.08830E-01	2.07999E-01	2.06296E-01
Y_{O_2}	5.74012E-06	6.27808E-06	1.89155E-05	4.07266E-05	9.76211E-05
Y_{NO}	9.37376E-04	9.98744E-04	2.15798E-03	3.67593E-03	6.76148E-03
ρ	7.74119E-04	7.64814E-04	6.97339E-04	6.52807E-04	6.04505E-04
p	2.10363E+03	2.09248E+03	2.07439E+03	2.06144E+03	2.04877E+03
T	5.77388E+03	5.82062E+03	6.43918E+03	6.93374E+03	7.58760E+03

Table 2: Solution at the stagnation point with chemical equilibrium

$v_y =$	100	1000	10000	32437	100000
Y_N	4.62112E-01	4.62173E-01	4.62272E-01	4.62344E-01	4.62414E-01
Y_{N_2}	3.27454E-01	3.27394E-01	3.27296E-01	3.27225E-01	3.27156E-01
Y_O	2.09498E-01	2.09499E-01	2.09501E-01	2.09502E-01	2.09503E-01
Y_{O_2}	5.67648E-06	5.66061E-06	5.63479E-06	5.61623E-06	5.59804E-06
Y_{NO}	9.30253E-04	9.28473E-04	9.25572E-04	9.23485E-04	9.21436E-04
ρ	7.58529E-04	7.54662E-04	7.48387E-04	7.43892E-04	7.39496E-04
p	2.10363E+03	2.09248E+03	2.07439E+03	2.06144E+03	2.04877E+03
T	5.76834E+03	5.76695E+03	5.76468E+03	5.76305E+03	5.76144E+03

Table 3: grid size $h = 0.5$ mm

	y_s	c	α	$y(x_1)$
ρ_N	0.19991273E-03	-0.80781548E-03	0.50471578E+00	0.18750639E-03
ρ_{N_2}	0.24793950E-03	-0.95975896E-03	0.10735826E+01	0.24776935E-03
ρ_O	0.11603159E-03	-0.33930816E-03	0.54705998E+00	0.11235681E-03
ρ_{O_2}	0.12330134E-06	0.91404103E-05	0.68942801E+00	0.15358958E-06
ρ_{NO}	0.65710286E-05	0.18052196E-03	0.60183032E+00	0.78083213E-05
ρE	0.13105287E+05	-0.30289441E+05	0.53345421E+00	0.12737924E+05
p	0.20906855E+04	-0.18559110E+10	0.33461180E+01	0.20983123E+04
T	0.81988008E+04	0.26001293E+05	0.53462722E+00	0.85099693E+04
$T_{\rho E} = 8159.0117047686$		$T_p = 8215.1801714935$		
$p_{\rho E} = 2076.3911117977$				

Table 4: grid size $h = 0.4$ mm

	y_s	c	α	$y(x_1)$
ρ_N	0.20305077E-03	-0.72739684E-03	0.48030513E+00	0.19079166E-03
ρ_{N_2}	0.24856616E-03	-0.25536107E-02	0.12226854E+01	0.24844406E-03
ρ_O	0.11710755E-03	-0.30859172E-03	0.52550932E+00	0.11356194E-03
ρ_{O_2}	0.11441500E-06	0.70641980E-05	0.64536941E+00	0.14354900E-06
ρ_{NO}	0.62547971E-05	0.14824280E-03	0.56566623E+00	0.74603221E-05
ρE	0.13208794E+05	-0.28025611E+05	0.51392267E+00	0.12853226E+05
p	0.20933196E+04	-0.61516578E+13	0.46129648E+01	0.20915281E+04
T	0.81167046E+04	0.21856474E+05	0.50024063E+00	0.84270561E+04
$T_{\rho E} = 8077.2888176093$		$T_p = 8144.9167960238$		
$p_{\rho E} = 2075.9385901421$				

Table 5: grid size $h = 0.3$ mm

	y_s	c	α	$y(x_1)$
ρ_N	0.20670728E-03	-0.65460752E-03	0.45455047E+00	0.19467365E-03
ρ_{N_2}	0.24931441E-03	-0.10356894E-01	0.14140019E+01	0.24922025E-03
ρ_O	0.11835569E-03	-0.28166107E-03	0.50305888E+00	0.11497124E-03
ρ_{O_2}	0.10479264E-06	0.52793397E-05	0.59661868E+00	0.13252049E-06
ρ_{NO}	0.59006480E-05	0.11795962E-03	0.52453868E+00	0.70693184E-05
ρE	0.13330360E+05	-0.26185338E+05	0.49414120E+00	0.12989828E+05
p	0.20942141E+04	0.0	0.0	0.20942141E+04
T	0.80234747E+04	0.18086707E+05	0.46289140E+00	0.83318977E+04
$T_{\rho E} = 7984.8015522491$		$T_p = 8040.9779384132$		
$p_{\rho E} = 2075.6566020433$				

Table 6: grid size $h = 0.2$ mm

	y_s	c	α	$y(x_1)$
ρ_N	0.20985258E-03	-0.58542245E-03	0.42479201E+00	0.19808780E-03
ρ_{N_2}	0.24995967E-03	-0.62566174E-01	0.16222580E+01	0.24987678E-03
ρ_O	0.11941402E-03	-0.25665548E-03	0.47629982E+00	0.11619809E-03
ρ_{O_2}	0.96633206E-07	0.38336304E-05	0.53939283E+00	0.12339933E-06
ρ_{NO}	0.55898729E-05	0.90948968E-04	0.47507639E+00	0.67378999E-05
ρE	0.13432646E+05	-0.24585223E+05	0.47111598E+00	0.13109328E+05
p	0.20962881E+04	0.0	0.0	0.20962881E+04
T	0.79406171E+04	0.14697074E+05	0.41978406E+00	0.82493746E+04
$T_{\rho E} = 7903.7673074697$		$T_p = 7971.0347446921$		
$p_{\rho E} = 2074.5185248101$				

Table 7: grid size $h = 0.1$ mm

	y_s	c	α	$y(x_1)$
ρ_N	0.21507150E-03	-0.51780233E-03	0.38734202E+00	0.20384577E-03
ρ_{N_2}	0.25070684E-03	-0.17829806E+01	0.19560081E+01	0.25062490E-03
ρ_O	0.12109627E-03	-0.23471594E-03	0.44302758E+00	0.11815857E-03
ρ_{O_2}	0.84567824E-07	0.24651723E-05	0.46512069E+00	0.10926742E-06
ρ_{NO}	0.51118945E-05	0.63458194E-04	0.41009834E+00	0.62079810E-05
ρE	0.13604307E+05	-0.23551882E+05	0.44259925E+00	0.13308085E+05
p	0.20991617E+04	0.0	0.0	0.20991617E+04
T	0.78111787E+04	0.11163308E+05	0.36365140E+00	0.81166359E+04
$T_{\rho E} = 7780.1129582163$		$T_p = 7860.4579352647$		
$p_{\rho E} = 2073.6480970424$				

Table 8: grid size $h = 0.1$ mm				
	y_s	c	α	$y(x_1)$
ρ_N	0.17984419E-03	-0.67378885E+00	0.17723435E+01	0.17984100E-03
ρ_{N_2}	0.25015325E-03	0.0	0.0	0.25008600E-03
ρ_O	0.11043832E-03	-0.89543947E-01	0.16425622E+01	0.11043800E-03
ρ_{O_2}	0.18671217E-06	0.14488872E-01	0.20010622E+01	0.18676900E-06
ρ_{NO}	0.89382853E-05	0.52574927E+00	0.20168725E+01	0.89403600E-05
ρ_E	0.12537008E+05	-0.49253741E+07	0.15647586E+01	0.12537000E+05
p	0.21027970E+04	0.0	0.0	0.21027907E+04
T	0.87257659E+04	0.88344790E+08	0.19920473E+01	0.87262245E+04
$T_{\rho E} = 8725.1529634401$		$T_p = 8728.3024435533$		
$p_{\rho E} = 2102.7258393496$				

B Figures

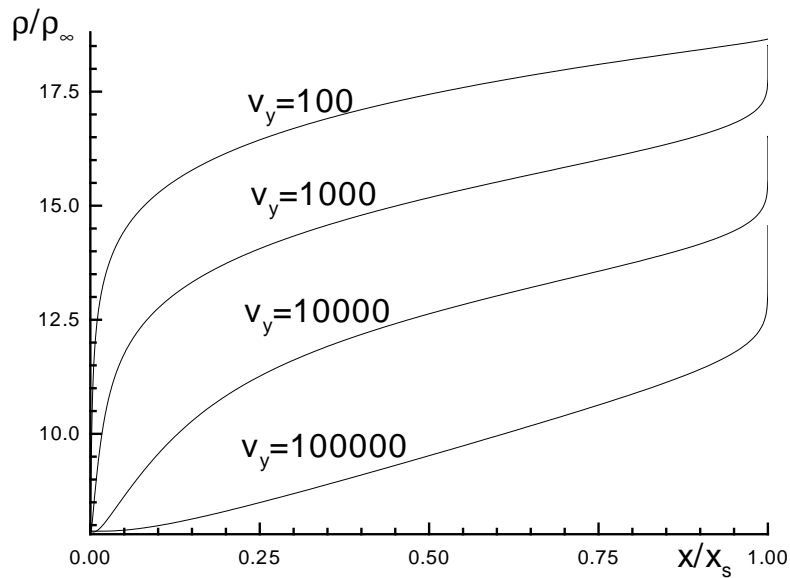


Figure 4: Density along the stagnation point streamline

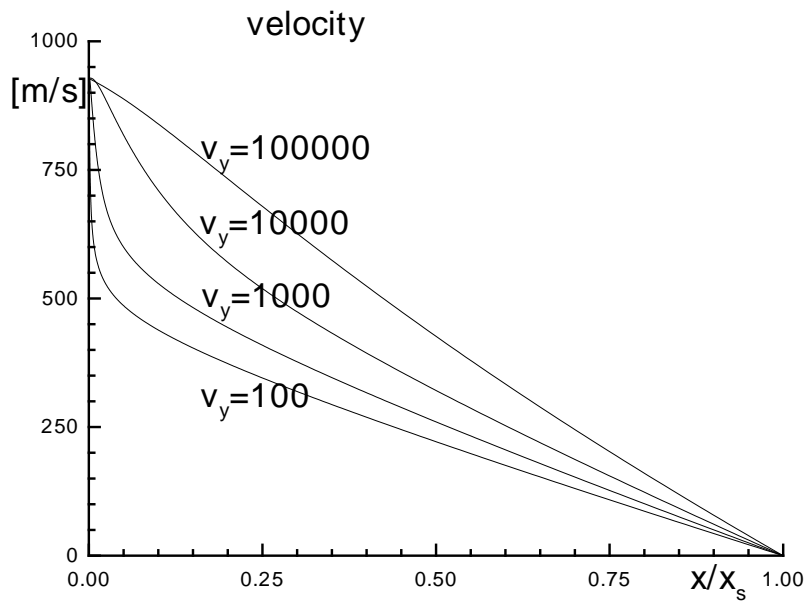


Figure 5: Velocity along the stagnation point streamline

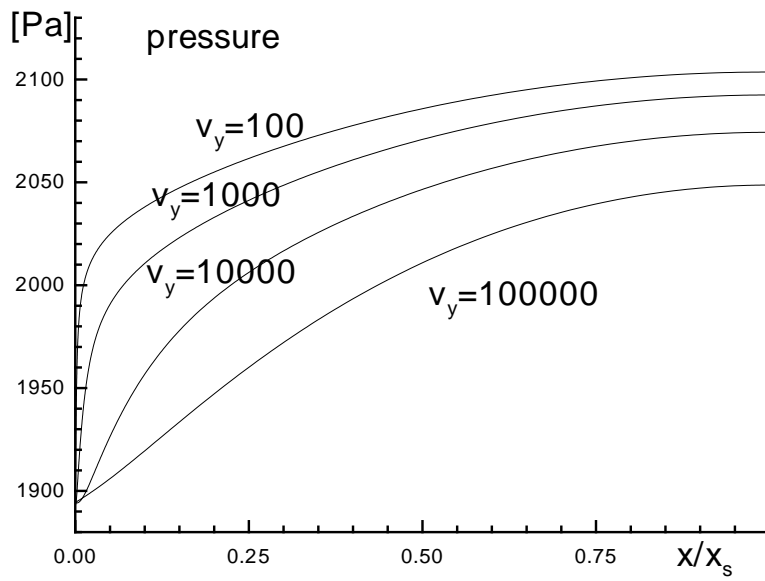


Figure 6: Pressure along the stagnation point streamline

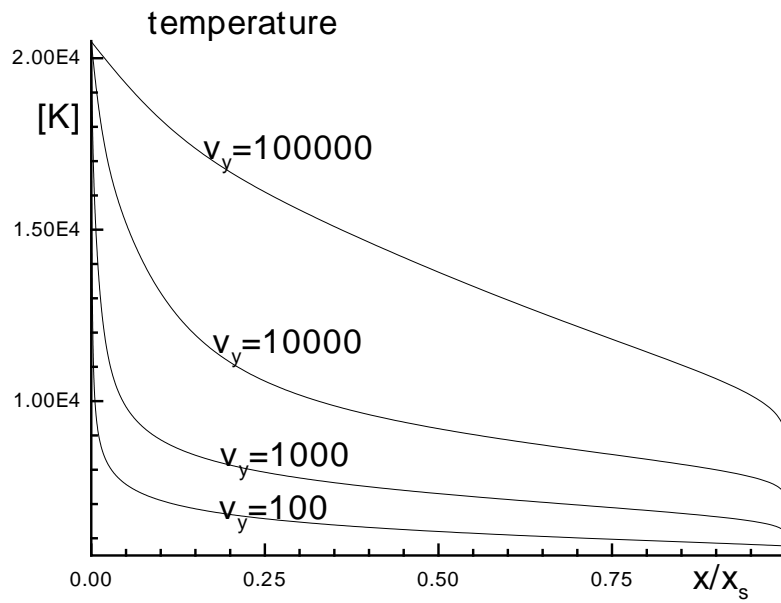


Figure 7: Temperature along the stagnation point streamline

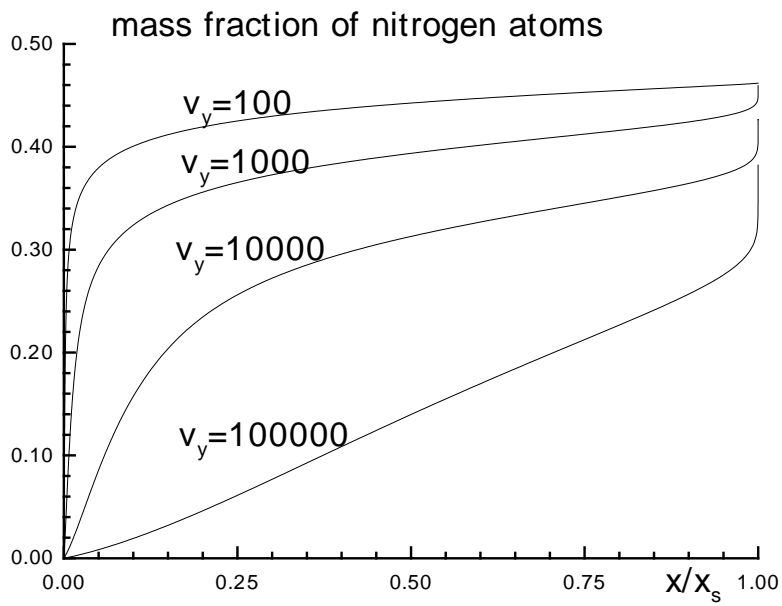


Figure 8: Mass fraction of nitrogen atoms along the stagnation point streamline

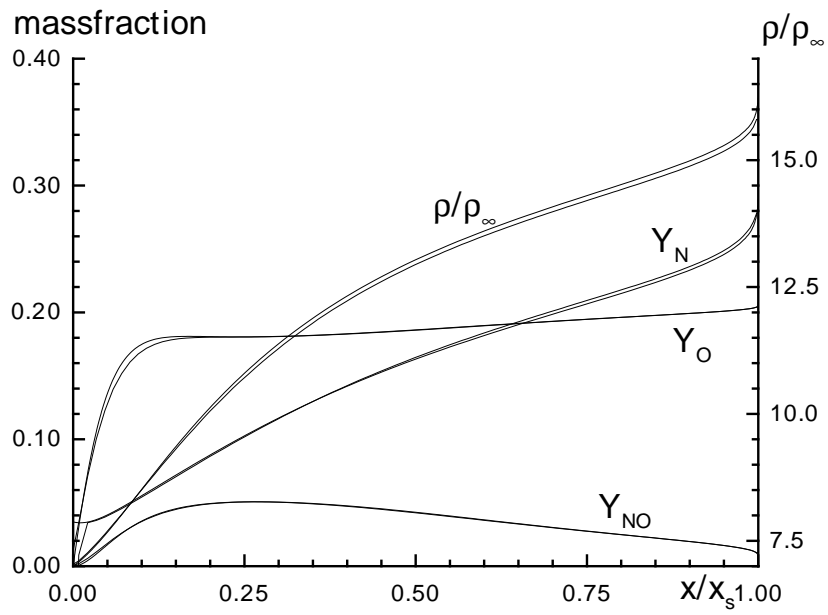


Figure 9: Comparison of solutions of BVP and 2D calculation

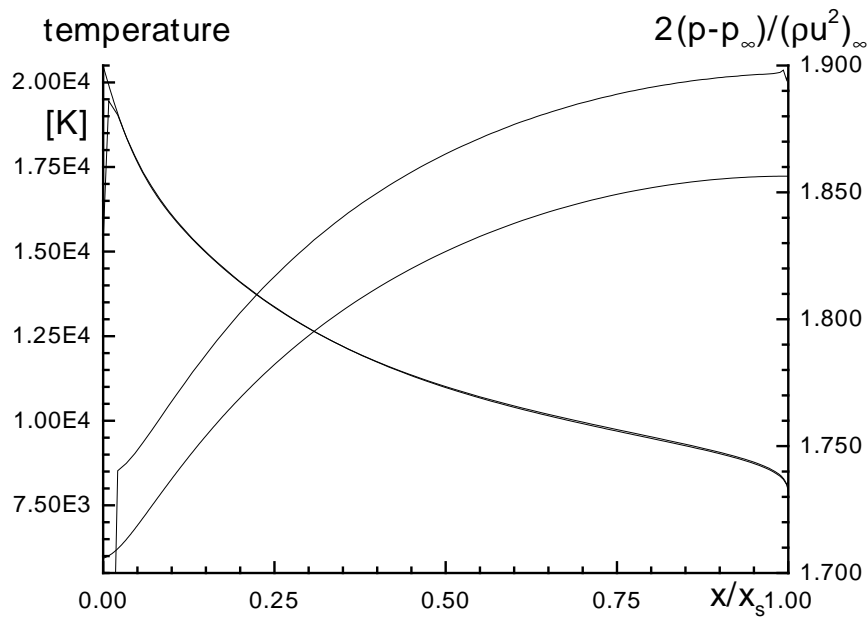


Figure 10: Comparison of solutions of BVP and 2D calculation

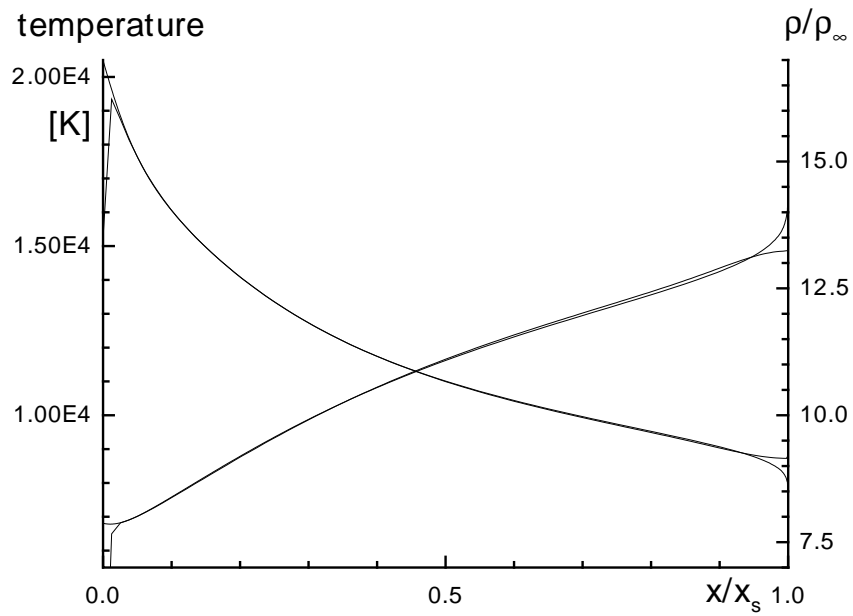


Figure 11: Comparison of solutions of BVP and 2D calculation with standard van Leer scheme

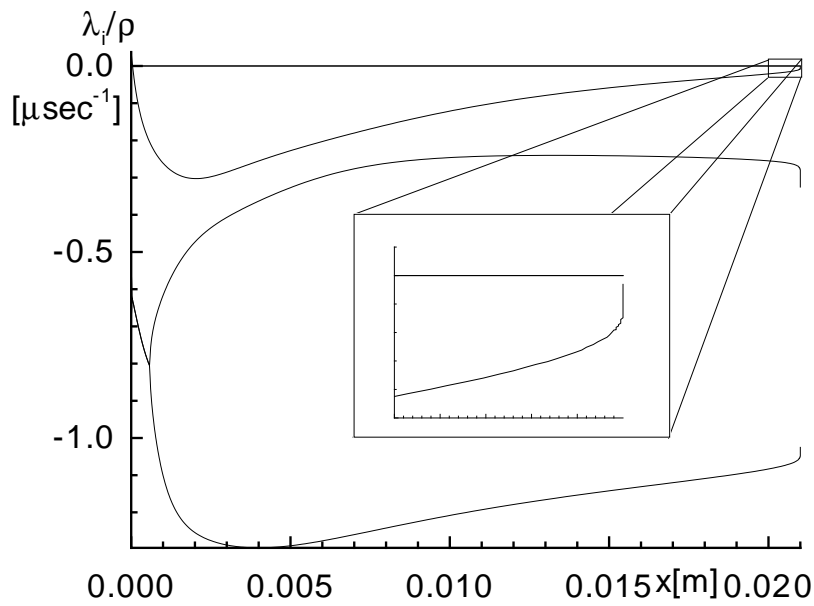


Figure 12: Real part of the eigenvalues along the stagnation point streamline

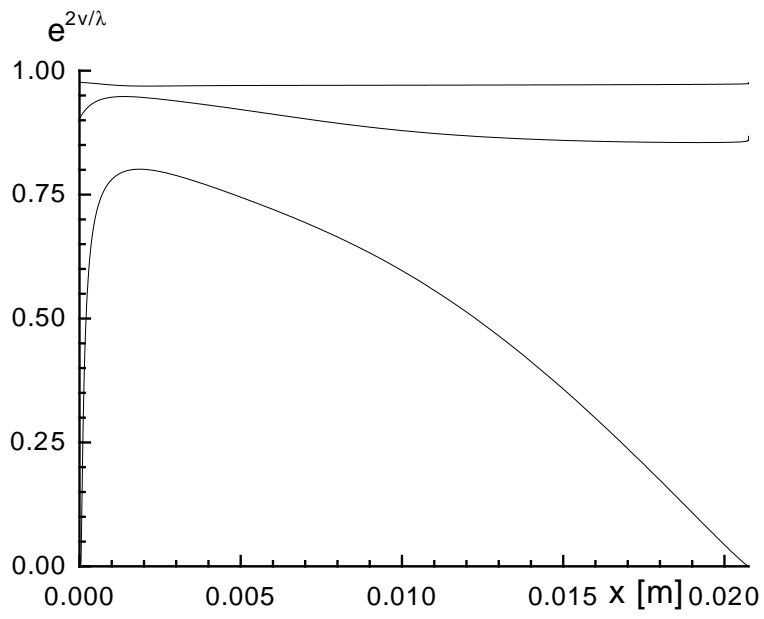


Figure 13: The function $\exp(2v_y/\lambda(x))$ for the real part of the eigenvalues along the stagnation point streamline

Research Reports

No.	Authors	Title
92-12	D. Mao	A Shock Tracking Technique Based on Conservation in One Space Dimension
92-11	K. Nipp, D. Stoffer	Attractive invariant manifolds for maps: Existence, smoothness and continuous dependence on the map
92-10	M. Fey, R. Jeltsch	A Simple Multidimensional Euler Scheme
92-09	M. Fey, R. Jeltsch	A New Multidimensional Euler Scheme
92-08	M. Fey, R. Jeltsch, P. Karmann	Numerical solution of a nozzle flow
92-07	M. Fey, R. Jeltsch, P. Karmann	Special aspects of reacting inviscid blunt body flow
92-06	M. Fey, R. Jeltsch, S. Müller	The influence of a source term, an example: chemically reacting hypersonic flow
92-05	N. Botta, J. Sesterhenn	Deficiencies in the numerical computation of nozzle flow
92-04	Ch. Lubich	Integration of stiff mechanical systems by Runge-Kutta methods
92-03	M. Fey, R. Jeltsch, S. Müller	Stagnation point analysis
92-02	C. W. Schulz-Rinne, J. P. Collins, H. M. Glaz	Numerical Solution of the Riemann Problem for Two-Dimensional Gas Dynamics
92-01	R. J. LeVeque, K. M. Shyue	Shock Tracking Based on High Resolution Wave Propagation Methods
91-10	M. Fey, R. Jeltsch	Influence of numerical diffusion in high temperature flow
91-09	R. J. LeVeque, R. Walder	Grid Alignment Effects and Rotated Methods for Computing Complex Flows in Astrophysics
91-08	Ch. Lubich, R. Schneider	Time discretization of parabolic boundary integral equations
91-07	M. Pirovino	On the Definition of Nonlinear Stability for Numerical Methods
91-06	Ch. Lubich, A. Ostermann	Runge-Kutta Methods for Parabolic Equations and Convolution Quadrature
91-05	C. W. Schulz-Rinne	Classification of the Riemann Problem for Two-Dimensional Gas Dynamics
91-04	R. Jeltsch, J. H. Smit	Accuracy Barriers of Three Time Level Difference Schemes for Hyperbolic Equations
91-03	I. Vecchi	Concentration-cancellation and Hardy spaces
91-02	R. Jeltsch, B. Pohl	Waveform Relaxation with Overlapping Splittings